JOURNAL OF NANO- AND ELECTRONIC PHYSICS
Vol. **4** No 1, 01008(4pp) (2012)

ЖУРНАЛ НАНО- ТА ЕЛЕКТРОННОЇ ФІЗИКИ
Том **4** № 1, 01008(4cc) (2012)

Corrosion Resistance of AZ91 Magnesium Alloy with Pulse Electrodeposited Ni-SiC Nanocomposite Coating

M. Hajiali Fini, A. Amadeh*

School of Metallurgy and Materials Engineering, College of Engineering, University of Tehran, Tehran, Iran

(Received 10 October 2011; published online 14 March 2012)

Magnesium and its alloys are the lightest of the structural metals, which makes them one of the most promising materials to minimize vehicle weight, but poor surface properties restrict the application of these alloys. In this paper, Ni-SiC nanocomposite coatings were applied on AZ91 magnesium alloy from Watts bath containing different amounts of SiC content by pulse electrodeposition technique. The morphology and phase analysis were carried out by Scanning Electron Microscopy (SEM) and X-Ray Diffraction (XRD) analysis, respectively. Microhardness of specimens was measured and the results revealed a significant enhancement from 74 H for bare AZ91 magnesium alloy to 523 HV for the specimen coated in the bath containing 15 $g.L^{-1}$ SiC. The Corrosion behavior of the samples was studied by potentiodaynamic polarization, and the obtained data showed superior corrosion resistance for coated AZ91 magnesium alloy, i.e. the corrosion current density decreased from 2.69 $mA.cm^{-2}$, for the uncoated sample, to 0.00046 $mA.cm^{-2}$, for coated specimen in the bath containing 15 $g.L^{-1}$ SiC and the corrosion potential increased from – 2.069 V to – 0.33 V at the same conditions.

Keywords: Nanocomposite coating, Pulse electrodeposition, SiC, Corrosion resistance, Microhardness.

PACS numbers: 81.07.Bc

1. INTRODUCTION

Due to high specific strength of magnesium, magnesium and magnesium alloys are being widely used in automotive and other industries [1]. However, the application of these alloys has been restricted because of the poor corrosion properties. The corrosion resistance improvement of these alloys has been subjected to a lot of researches in recent years [2]. Application of appropriate coatings, such as Ni, Cr etc., on these alloys is one the most applicable procedures for improving the corrosion behavior of magnesium [3, 4]. These coatings can be reinforced by ceramic particles such SiC, Al_2O_3, TiO_2 etc. [5-7]. In particular, during recent years, Ni–SiC composites have been widely investigated and successfully commercialized in the automotive and aerospace industry as a result of their improved mechanica and tribological properties[8]. Also the Ni-SiC composite coatings, is one the most promising corrosion resistant coatings which have been used on different alloys [9, 10].

With the increasing availability of nano-particles, the interest for electrolytic and electroless composite coatings containing nano-particles is growing [11]. The major challenges with the codeposition of nanoparticles are the achievement of a high level of codeposition, and avoidance of the agglomeration of ceramic particles suspended in the electrolytes. It has been found that appropriate selection of pulse current parameters led to the achievement of Ni-SiC coatings with higher incorporation and more uniform distribution of ceramic particles in the metallic matrix, which resulted in better properties with respect to direct current technique [12-14].

In this study, the corrosion improvement of AZ91 magnesium alloy by application of Ni-SiC nano composite coating was investigated. For this aim, different coatings, from solution with different SiC content, were applied on the alloy and the Corrosion behavior of each one was studied.

2. METHODS OF SAMPLE MANUFACTURING AND ANALYSIS

The substrate material used was AZ91 as cast magnesium alloy with a size of 20 mm × 20 mm × 5 mm. The chemical composition of the alloy is given in Table 1. The samples were abraded with No. 2000 SiC paper before the pretreatment processes. The Zinc immersion coating was used as the pretreatment [15].

Table 1 – Chemical composition of AZ91 magnesium alloy

Al (wt.%)	Zn (wt.%)	Mn (ppm)	Fe (ppm)	Mg
9	1	0.17	0.01	Balance

The coatings were prepared from Watts solution. The Ni-SiC layers was electrodeposited from a suspension of SiC nano-particles with average grain size of 40 nm in the bath (Fig. 1). The bath composition as well as operating conditions are shown in Table 2. To adjust the pH of the bath, NaOH and H_2SO_4 were used for increasing and decreasing, respectively.

Electrodeposition of Ni-SiC composite coatings was performed by using square pulse current in which the duty cycle is defined as $T_{on}/(T_{on}+T_{off})$, where T_{on} is the on-time period and T_{off} is the off-time period of imposed pulses. After two hours of electroplating, the thickness of coatings was measured as 30 μm.

SEM investigations were carried out using a Philips XL30 instrument on the samples while a thin layer of gold was deposited on them.

XRD investigations were conducted using a Philips X'PertPro instrument with CuKα radiation. Potentiodynamic polarization tests were performed by suspending the samples in 3.5 wt.% NaCl solution. The counter and reference electrodes were platinum and Saturted Calomel Electrode (SCE), respectively. After

* amedeh@ut.ac.ir

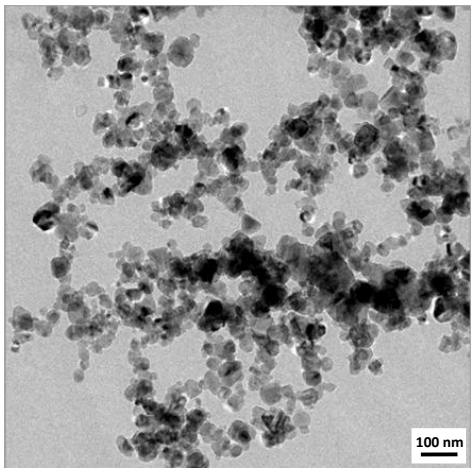

Fig. 1 – TEM photograph of SiC particles (curtsey of Hefei Kaier Nanometer Energy & Technology Co., Ltd)

Table 2 – Chemical composition and operating conditions of electroplating solution

Item	Value
$NiSO_4.7H_2O$	300 $g.L^{-1}$
$NiCl_2.6H_2O$	45 $g.L^{-1}$
H_3BO_3	45 $g.L^{-1}$
Saccharin	1 $g.L^{-1}$
Sodium Dodecyl Sulfate (SDS)	1 $g.L^{-1}$
Current density	50 $mA.cm^{-2}$
pH	4.5
Temperature	50 °C
Frequency	10 Hz
Duty Cycle	30 %
SiC	0, 10, 15 $g.L^{-1}$

about one hour stabilization at rest potential, polarization test commenced at a scan rate of 1 mV/s using an EG&G273 instrument. The corrosion current density was determined by varying ± 20 mV around the E_{OCP}. Vickers microhardness of magnesium alloy and coatings were evaluated using a Vickers microhardness tester at a load of 200 g and duration of 30 s. For each specimen, the average hardness value was taken from at least 3 tests.

3. RESULTS AND DISCUSSION

3.1 Microstructure

The typical XRD pattern of the coating applied from the bath containing 10 $g.L^{-1}$ SiC is illustrated in Fig. 2. It shows the typical peaks of Ni with peaks of (111), (200) and (220). The other peaks are corresponding to the copper which applied as the undercoating and Magnesium, the substrate.

The surface morphology of coatings at different magnifications is shown in Fig. 4a-f. The nickel coating has covered the whole surface of the substrate and SiC nanoparticles are uniformly distributed in metallic matrix. Although the agglomeration of SiC particles has occurred, but it is not considerable. It can be seen that the coatings are compact and uniform with no microcracks.

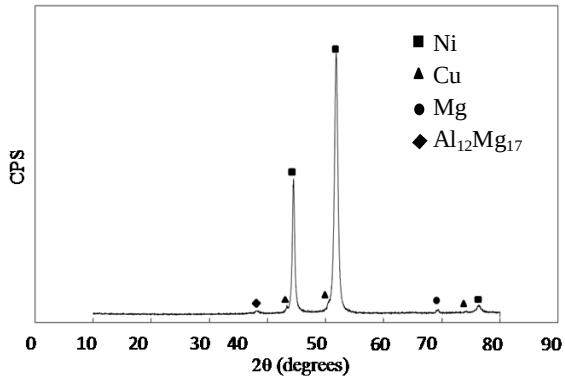

Fig. 2 – XRD pattern of Ni-SiC coating applied from the bath containing 10 $g.L^{-1}$ SiC

The cross section of coated AZ91 is shown in Fig. 3. No abortions or cracks are observed along the interface of the substrate and the coating, and therefore, good adhesion between the coating and the substrate is expected.

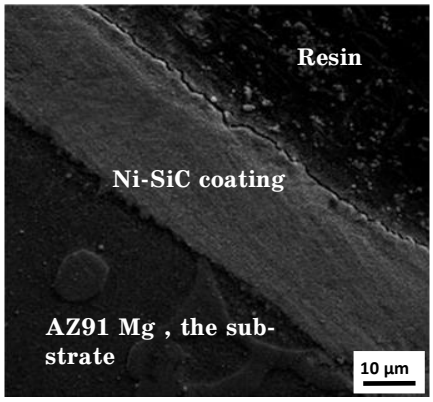

Fig. 3 – SEM image of cross section of coated AZ91

Fig. 5. It can be seen that application of pure Ni coating enhances significantly the hardness of AZ91 alloy and codeposition of SiC particles leads to further improvement of the hardness. As the SiC concentration in the bath increases, the microhardness of coating improves too. This could be attributed to the embedded SiC volume fraction. Kim and Yoo [16] suggest that in the used range of SiC concentration in the bath, as the amount of SiC particles increases in the bath, more SiC will cooperate in the coatings.

The reason why the microhardness of the Ni-SiC nanocomposite coatings is higher than the Ni coating is that the SiC nano-particulates uniformly distributed in the Ni matrix could restrain the growth of the Ni alloy grains and the plastic deformation of the matrix under a loading, by way of grain fining and dispersive strengthening effects. The grain fining and dispersive strengthening effects become stronger with increasing SiC nano-particulates content in composite coatings, thus the microhardness of the Ni–SiC composite coatings increases with the increase of SiC particulates content.

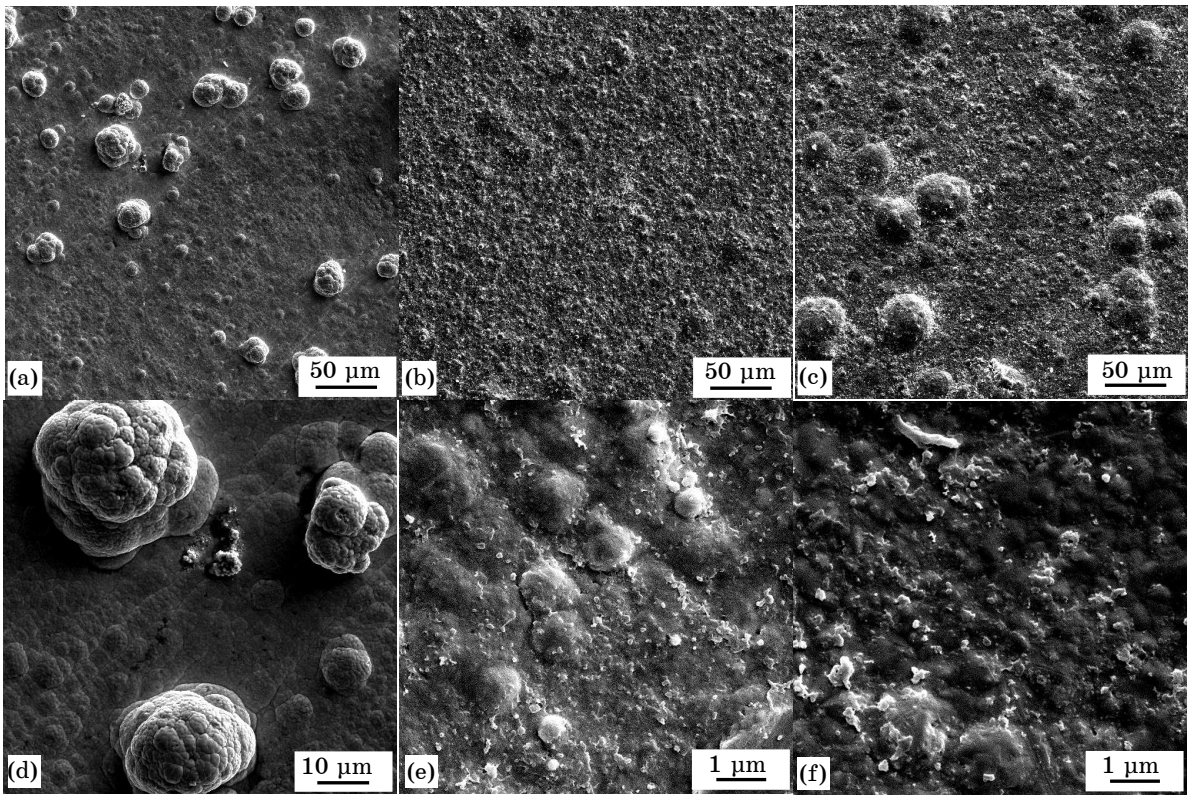

Fig. 4 – SEM micrographs of Ni-SiC coatings applied from the baths containing: (a,d) 0 $g.L^{-1}$ SiC, (b,e) 10 $g.L^{-1}$ SiC, (c,f) 15 $g.L^{-1}$ SiC

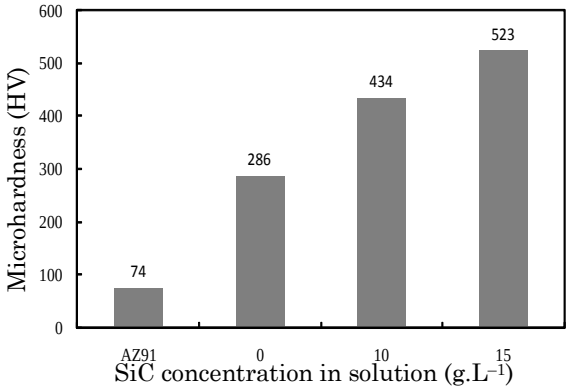

Fig. 5 – Variation of microhardness of the coatings as a function of SiC concentration in the bath

3.2 Corrosion

Potentiodaynamic polarization curves of bare and coated substrates are presented in Fig. 6. As it is seen, the application of Ni-SiC coating improves the corrosion resistance of AZ91 alloy and the embedded SiC nano-particles lead to considerable reduction in the corrosion current density and also shift the corrosion potential to more positive values.

The polarization data has been brought in Table 3. As it can be discern the corrosion current density of bare substrate decreased from 2.69 $mA.cm^{-2}$ to 0.16, 0.012 and 0.00046 $mA.cm^{-2}$, for the coated samples from the bath containing 0, 10 and 15 $g.L^{-1}$, respectively. In addition, the corrosion potential, increased from –2.069 for the bare substrate to –1.23, –0.41 and –0.33 for the coated samples from the bath containing 0, 10 and 15 $g.L^{-1}$, respectively.

The Ni coating acts as the barrier against the corrosive materials and protects the substrate. The present of the SiC particles leads to the considerable corrosion resistance improvement and as the SiC concentration in the bath increases the corrosion resistance enhanced. This trend is due to the enhancement of the embedded SiC nano particles. The roles of SiC particles in this improvement can be stated as follow:

1) Ceramic particles such as SiC, WC and Al_2O_3 have a good corrosion resistance and the presence of these particles in the coating enhances the corrosion resistance. When these particles are distributed in the coating, the area of the coating in contact with corrosive media reduces. Thus, the codeposition of SiC particles in the coating improves its corrosion resistance.

2) SiC particles distributed in the nickel matrix act as the barriers which can change the corrosion path and even prevent its progress.

3) Codeposition of SiC particles in the nickel coating can change its morphology from a columnar morphology to a coaxial one. In a columnar morphology there are the straight paths that corrosion can take place readily and fast through them. But in a coaxial morphology, the straight and long paths are substituted with short and meandrous ones which lead to a decline in corrosion rate.

4) The presence of SiC nano-particles reduces the submicron defects of the coating and restricts the access passages of corrosive media to the coating surface.

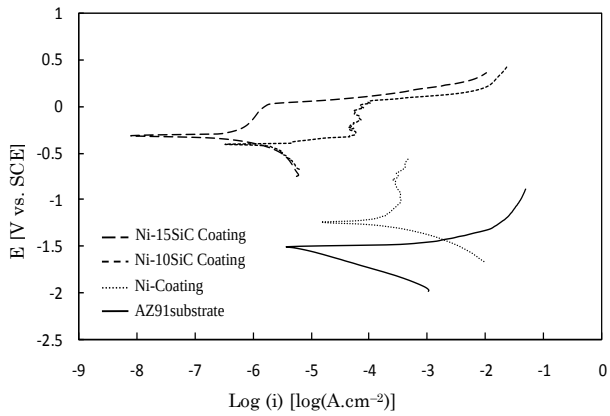

Fig. 6 – Polarization curves of bare magnesium alloy substrate, pulse electrodeposited Ni coating, Ni-10SiC (doposited from the bath containing 10 g.L^{-1} SiC) and Ni-15SiC (doposited from the bath containing 15 g.L^{-1} SiC) nanocomposite coating in 3.5 wt.% NaCl solution

Table 3 – Polarization data calculated from Fig. 6

		SiC concentration in the bath (g.L^{-1})		
	AZ91	**0**	**10**	**15**
I_{corr} (mA.cm^{-2})	2.69	0.16	0.0012	0.00046
E_{corr} (V vs. SCE)	–2.069	–1.23	–0.41	–0.33

4. CONCLUSIONS

To improve the corrosion resistance of AZ91 magnesium alloy, Ni and Ni-SiC nanocomposite coatings were applied on the alloy by pulse electrodeposition. The major results attained from experimental studies can be summarized as:

- The microhardness of bare AZ91 alloy was 74 HV, and increased to 523 HV for the coating applied from the bath containing 15 g.L^{-1} SiC.
- The corrosion potential increased from –2.069 V, for AZ91 alloy to – 0.33 V for the coating applied from the bath containing from 15 g.L^{-1} SiC.
- The corrosion current density reduced, i.e. the corrosion resistance of coated AZ91, improved about 5600 %.

REFERENCES

1. B.L. Mordike, T. Ebert, Mater. *Sci. Eng. A* **302**, 37 (2001).
2. Zhong-Hou Li, Zhi-Yong Chen, Sha-Sha Liu, Feng Zheng, A-Gan Dai, *T. Nonfer Metal. Soc.* **18**, 819 (2008).
3. Changdong Gu, Jianshe Lian, Guangyu Li, Liyuan Niu, Zhonghao Jiang, *J. Alloy. Compd.* **391**, 104 (2005).
4. W.X. Zhang, N. Huang, J.G. He, Z.H. Jiang, Q. Jiang, J.S. Lian, *Appl. Surf. Sci.* **253**, 5116 (2007).
5. A. Araghi, M.H. Paydar, *Mater. Design* **31**, 3095 (2010).
6. P. Rodrigo, M. Campo, B. Torres, M.D. Escalera, E. Otero J. Rams, *Appl. Surf. Sci.* **255**, 9174 (2009).
7. Shiyan Zhang, Qing Li, Xiaokui Yang, Xiankang Zhong, Yan Dai, Fei Luo, *Mater. Charact.* **61**, 269 (2010).
8. F. Hu, K.C. Chan, *Appl. Surf. Sci.* **233**, 163 (2004).
9. K.H. Hou, M.D. Ger, L.M. Wang, S.T. Ke, *Wear* **253**, 994 (2002).
10. A.F. Zimmerman, D.G. Clark, K.T. Aust, U. Erb, *J. Mater. Lett.* **52**, 85 (2002).
11. Y.V. Timoshkov, I. S. Molchan, S. V. Labunov, V. I. Kurmashev, T. M. Gubarevich, J. Fransaer, J. P. Celis, *Surface Modification Technologies*, Institute of Materials, London **11**, 991 (1998).
12. P. Gyftou, E.A. Pavlatou, N. Spyrellis, K.S. Hatzilyberis, *Trans. Inst. Met. Finish.* **78**, 223 (2000).
13. G. Maurin, A. Lavanant, *J. Appl. Electrochem.* **25**, 1113 (1995).
14. S. Psarrou, P. Gyftou, E. Pavlatou, C. Kollia, N. Spyrellis, Proc. *Interfinish 2000, Garmisch Partenkirchen, Germany, September* (2000).
15. Standard Test Method for Preparation of Magnesium and Magnesium Alloys for Electroplating, ASTM B480, Annual Book of ASTM Standards, vol. 02.05, American Society for Testing and Materials, West Conshohocken, PB, (2003).
16. Sun Kyu Kim, Hong Jae Yoo, *Surf. Coat. Tech.* **108-109**, 564 (1998).